



# Modelling of inductive wireless charging for electric vehicles

Krzysztof Jakubiak 

Jun Liang 

Liana Cipcigan

**Abstract**—In response to government’s global warming targets, electric vehicles (EV) penetration is increasing rapidly. To support the uptake of EVs and facilitate their charging demands, the charging technology and infrastructure also need to be developed. In this paper, the modelling of a wireless power transfer (WPT) system is developed considering a static scenario and then adapting the model for a dynamic charging scenario. This research work is aiming to replace previously used transformer approximation of WPT, before adapting the model for dynamic charging. Using the proposed implementation, it is possible to easily vary system parameters, design and control, providing a solid foundation for future research. The resulting model uses a pair of inductive coils and allows full control over coil misalignment (in three dimensions), further facilitating the use of variable misalignment for dynamic application.

**Index Terms**—Electric vehicle, Dynamic, Wireless charging

## I. INTRODUCTION

In order to reach global climate change targets of 1.5°C [1,2], different sectors and industries require decarbonisation. UK government has committed to reducing emissions by 78% by 2035 [4]; becoming a milestone toward reaching their goals of becoming a net zero emissions nation by 2050 [5]. To reduce the emission from transport sector, the UK government banned the sale of new petrol and diesel cars by 2030 and the sale of hybrids from 2035. The ambition is to all new cars and vans be fully zero emission at the tailpipe from 2035 [6], as the transport sector is the largest-emitting sector accounting for 23% of UK emissions [3]. As freight and road transport continue to grow the transport sector is forecast to continue increasing its environmental impact, therefore it is important to see technological advancements to support decarbonisation and meet the aforementioned targets.

With the increased uptake of electric vehicles (EVs) across various sectors of transportation, charging technologies are also receiving increased attention to provide viable solutions to meet demand, increase output power and quality. Most currently available charging solutions are conductive (plug-in) chargers, most commonly available in the range of 3-50kW for currently available vehicles. With 50-80% of charging events taking place at residential homes [7], and 35% of EV drivers charging at home with off-street parking [8]. This requires the user to install a charger at home, increasing the initial cost of ownership for EVs, likewise workplaces also have this cost associated to provide their employees with charging solutions. In the future with higher market penetration this will also increase the power demand on distribution grids, leading to necessary system upgrades. Conductive plug-in chargers require the user to stop at a designated location to charge,

resulting in waiting times which for some sectors such as freight or public transport will become a point of concern when adopting EVs. One option is to use wireless power transfer (WPT) solutions which are based on a magnetic field created by primary inductive coil (on the ground or in the road surface), which in turn induces a voltage on the secondary coil (on the vehicle) resulting in WPT.

Static WPT chargers are able to achieve >90% efficiency [9] with different alignment and air gap tolerances. However, for peak efficiency the displacements between the coils can be designed around, for the system to function at (or close to) resonance. Static WPT solutions still require the user to park in a designated area, over a charging pad, however they do provide the convenience of not having to plug-in manually, reducing the amount of equipment taking up space on the roadside, driveway or garage. The dynamic wireless power transfer (DWPT) is similar with the wireless static charging but with multiple chargers’ side by side, allowing vehicles to drive over while charging. During DWPT, power transfer for a pair of coils varies over time as the receiving coil moves over the transmitting coil and therefore using an array of transmitting coils can provide WPT over a longer distance. Implementing a dynamic solution can reduce the frequency of charging stops or possibly eliminate it, overcoming the issues seen for larger vehicles. Applications of DWPT achieved system efficiency of 89.54% [10](up to 80kW) with lower power (400W) achieving up to 90.2% [11]. This drop in efficiency (compared to static WPT) is due to the dynamic nature of the system, where the mutual inductance between transmitter and receiver varies overtime, resulting in a reduction of the coupling coefficient, which describes power transfer between two coils as well as varying resonant frequency of the system reducing efficiency. Previous research and projects on DWPT present systems with multiple primary coils and one receiving coil [12]–[14].

Batteries require CC/CV modes depending on their state-of-charge (SOC), hence topological solutions aren’t ideal, hence control should be implemented on either the primary or secondary side of the system. Research for WPT shows the system can be designed to provide constant current (CC) or constant voltage (CV) characteristics using different compensation topologies [20] or with primary side control [21]. Existing models approximate the load (DC/DC converter and battery) to be a resistive one [22]. Commonly used approaches result in load dependant equations and in order to simplify the load (DC/DC converter and battery) is often taken as a constant the resistive load [23]–[25]. This approach allows system analysis and design at specific parameters. Previous

research focuses on step response of stationary systems which can be used as a first approach to the problem, however showing the dynamic response of the system is of interest for future research and better show of the system response.

This paper focuses on the modelling of DWPT systems, first introducing the basic system and working principles, followed by further expanding the wireless coupling between the coils as a function of displacement, before showing the model implementation for a dynamic system with control over vehicle speed and misalignment. This model was developed using MATLAB Simulink.

## II. MODEL EXPLANATION

### A. Theory Model

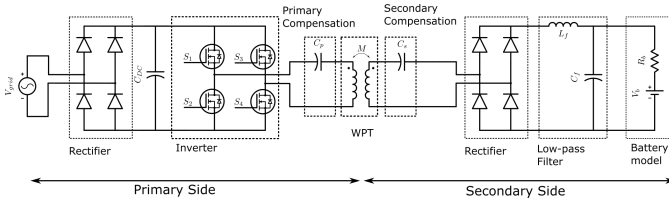


Fig. 1. Circuit diagram of WPT

The inductive power transfer model is approximated to function like a transformer, with the absence of a closed-core. Functionally the core provides a high mutual inductance between the two coils, allowing for more efficient power transfer, in the inductive WPT case, the mutual inductance is a function of position between the two coils. While different topologies can be used for AC & DC charging, this relies on high frequency inverters to maximise the power transferred while minimising compensation component size [26]. The link between primary and secondary side for WPT is the mutual inductance between the primary and secondary coils. Both coil parameters (resistance and inductance) remain the same with the exception of mutual inductance as this varies based on separation distance of the coils. For a dynamic case, the mutual inductance will: start to rise as the secondary coil (vehicle) approaches the primary coil; peak when the two coils are vertically aligned; decrease as the vehicle drives away from primary coil.

### B. Inverter

The H-bridge topology is commonly used for inverter design with differences in switches and passive components. One such application is the high frequency proposed for space stations [27], where the topology can be rearranged to show a H-bridge inverter connected to a passive LC filter. The H-bridge forms the basis for the most commonly used inverter topologies and the most common addition is a resonant network connection (an LC filter) to improve power quality of the output voltage [28]. A voltage source inverter is required to drive the WPT system at resonance for optimal power transfer. For this purpose, a full bridge inverter is used with sinusoidal PWM

control to drive the system at a fixed modulation index and frequency (both switching and reference). The reference signal frequency ( $f_{ref}$ ) should be set to the natural frequency of the power transfer coil and compensation.

### C. Inductive power transfer

Isolating the inductive coil part of the system, a high frequency sinusoidal input is expected to the primary coil, this creates an electromagnetic field (EMF) around the coil. As the secondary coil intersects the EMF a potential difference (voltage  $V_1$ ) is seen across the coil according to Lenz's law. This means the voltage ( $V_2$ ) induced in the is a function of the current in the secondary coil is a function of the primary coil current ( $I_1$ ), and vice versa as seen in Figure 2. The link between both coils is described by the mutual inductance such that:

$$M < \sqrt{L_1 L_2} \quad (1)$$

$$V_1 = -sMI_2 \quad (2)$$

$$V_2 = sMI_1 \quad (3)$$

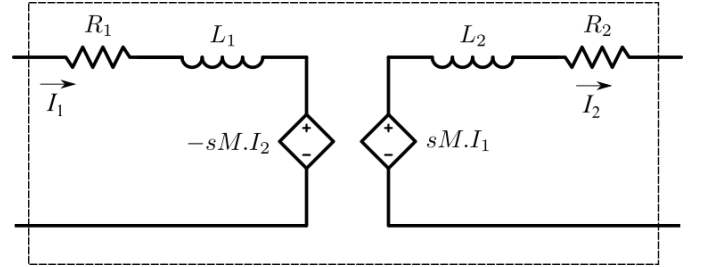


Fig. 2. Equivalent circuit for WPT coils

The mutual inductance between two coils is a function of their physical properties (their size, shape, material), the separation between both coils and the material between them (permeability) [16] and its equation can be seen in (A)1. To implement dynamic behaviour, the displacement of the coils is updated based on velocity, which is fed into equation (A) to find the value of mutual inductance over time for different position, hence achieving dynamic behaviour. Figure 3 shows the simulation implementation replacing the WPT block in Figure 1 to realize equations (2) and (3).

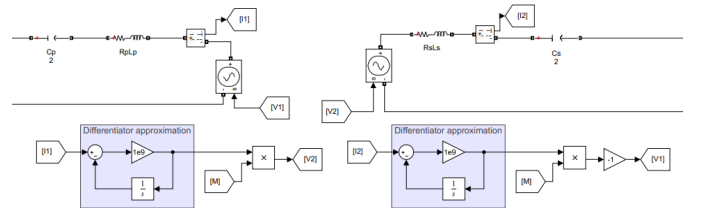


Fig. 3. WPT implementation

#### D. Compensation circuits

Designed to improve the power transfer characteristics of the model, the topology of compensation will impact the system characteristics. In this model a series-series (SS) compensation topology was used due to its high output power and efficiency as identified in literature [20]. Once topology is decided, the size of components is chosen according to coil inductance to match the resonance of both the secondary and primary circuits.

### III. MODEL SPECIFICATION

As mentioned in II-D, the model uses SS compensation and further models a pair of square coils due to ease of manufacture for later research.

#### A. Specification used

TABLE I  
SYSTEM SPECIFICATIONS

Input voltage		415 V
Inverter	Switching frequency	1 MHz
	Fundamental frequency	82 kHz
Primary side	Compensation capacitor	6.2969 $\mu\text{F}$
	Coil self-inductance	598.2 $\mu\text{H}$
	Coil resistance	177.8 m $\Omega$
Secondary side	Compensation capacitor	6.2297 $\mu\text{F}$
	Coil self-inductance	604.65 $\mu\text{H}$
	Coil resistance	192.6 m $\Omega$
LPF	Capacitor	1 mH
	Inductor	10 $\mu\text{F}$
	Cut-off frequency	1.59 kHz
Battery Specifications	Nominal Voltage	400 V
	Capacity	75 A h

Mutual inductance is a function of permeability, coil dimensions and coil displacements. As the coil parameters (e.g. size, inductance, shape) remain constant, further, in this model a constant permeability is assumed, using the permeability of free space. This may be different with the presence of rainfall, snow, ice or other materials. Mutual inductance then becomes a function of displacement of the two coils, such that  $M(x, y, z)$ .

### IV. RESULTS ANALYSIS AND COMPARISON

Changing system parameters affects the mutual inductance between primary and secondary coils. The change in mutual inductance is related to the resulting output power as an increase in mutual inductance leads to higher power transfer, the impact of varying different variables within the system is explored and the output power and mutual inductance is shown for each case. Primary and secondary coil width and height are 0.3m, an air gap of 0.3m as the parameters when designing the system. For most simulation a velocity of  $100\text{ms}^{-1}$  (224mph) is used to reduce simulation time, the impact of varying travel speed is also explored in Section IV-B.

#### A. Varying ride height

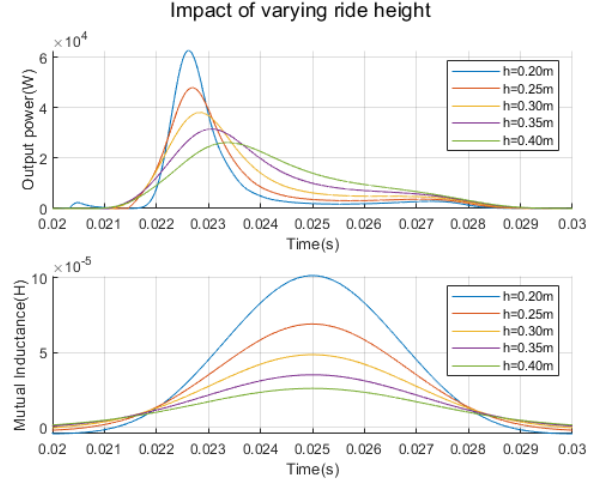


Fig. 4. Output power and mutual inductance over time.

The results in Figure 4 show the significant impact of ride height on mutual inductance and its resulting power transfer. While the ride height of a specific vehicle is not expected to change drastically, the height may vary for different types of vehicles (especially for laden transport vehicles). Hence this needs to be considered when designing a DWPT system.

#### B. Varying speed

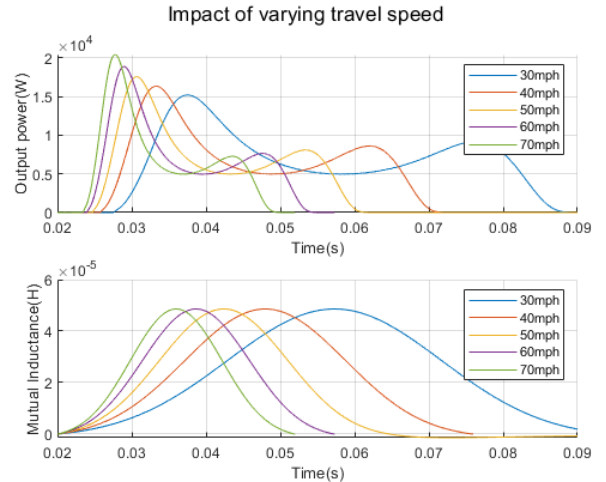


Fig. 5. Output power and mutual inductance over time for different travel speeds.

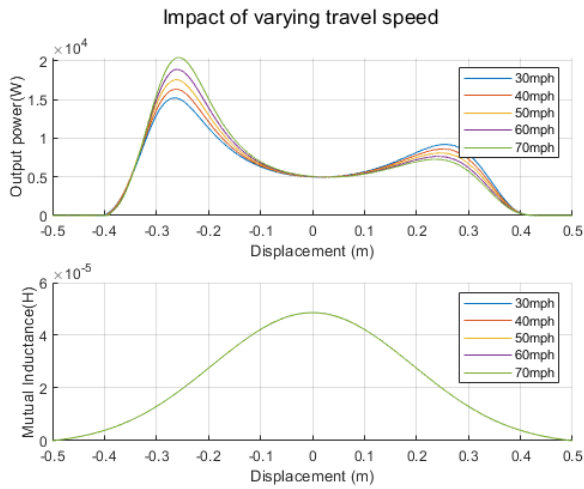


Fig. 6. Output power and mutual inductance over displacement for different travel speeds.

Figure 5 shows the effect of travelling at different constant velocities. As it is expected, lower velocities are able to stay at a higher value of mutual inductance for a longer period of time, resulting in a higher power transfer over the whole charging event. Figure 6 uses the relative displacement of the coils as opposed to time, verifying the simulation accuracy as mutual inductance is expected to be the same for a given position. This also shows the impact travel speed has on the instantaneous power in the system.

### C. Changing primary coil size

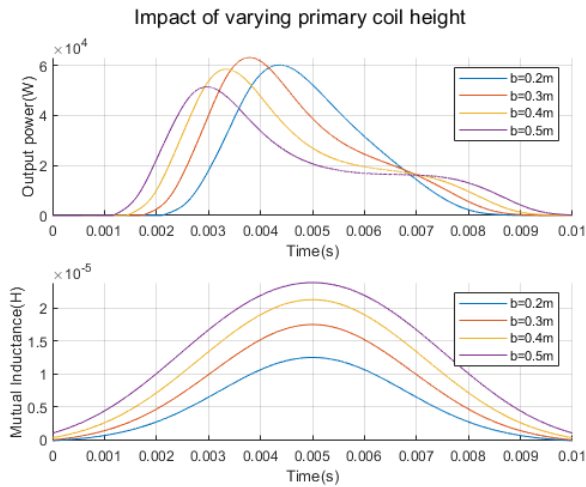


Fig. 7. Impact of varying primary coil height.

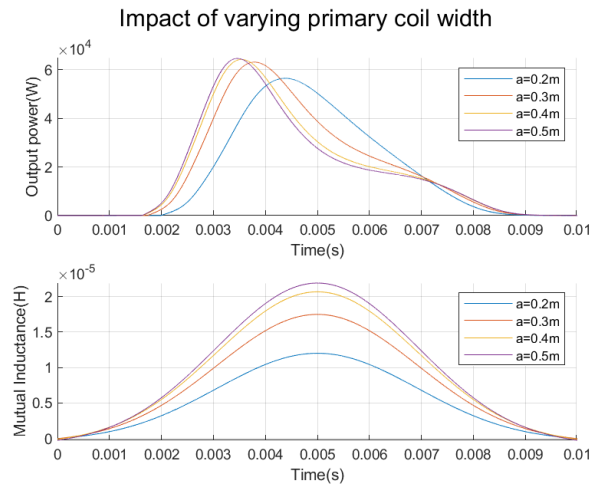


Fig. 8. Impact of varying primary coil width.

Figure 7 and 8 show the effect of changing the height and width of the primary coil respectively. Note, the simulation maintains the same operating frequency each time and has been optimised for a coil size of  $b=0.3\text{m}$  and  $a=0.4\text{m}$ . Hence variation is expected to transfer less power, even if mutual inductance is increased, as the increase/decrease in size will affect the inductance of the coil and therefore change the natural frequency of the system.

### D. Changing secondary coil size

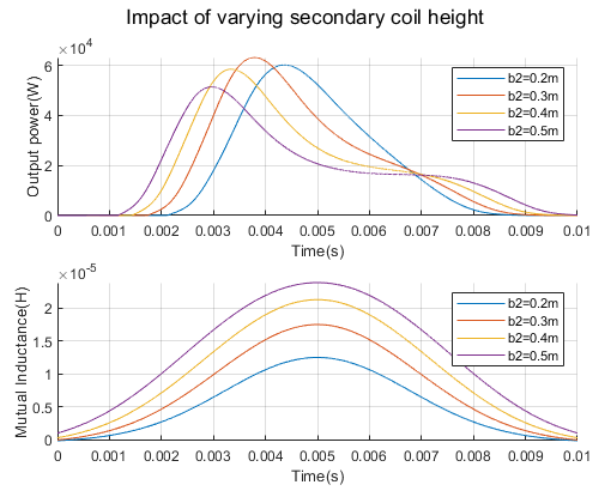


Fig. 9. Impact of varying secondary coil height.

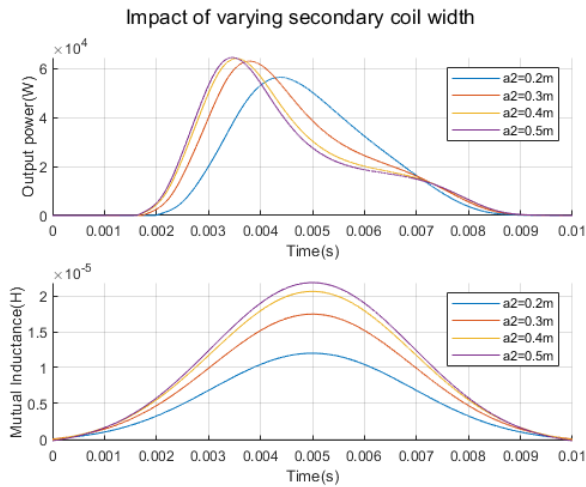


Fig. 10. Impact of varying secondary coil width.

Figure 9 and 10 show the effect of changing the height and width of the secondary coil respectively. Note, the simulation maintains the same operating frequency each time and has been optimised for a coil size of  $b=0.3m$  and  $a=0.4m$ . As for the primary coil the performance is expected to be lower when not operating at resonance.

#### E. Discussion

The mutual inductance model performs as expected, showing symmetrical behaviour as a function of lateral misalignment, as expected for a pair of symmetric coils. The peak value is also expected at zero misalignment, when the distances between coils is minimised, hence the receiver coil is in a region of maximum flux density. The presence of both aforementioned characteristics indicates the mutual inductance model is correct, and the resulting model is approximating the dynamic charging scenario. Other research in this field show similar waveforms for mutual inductance (Figure 11).

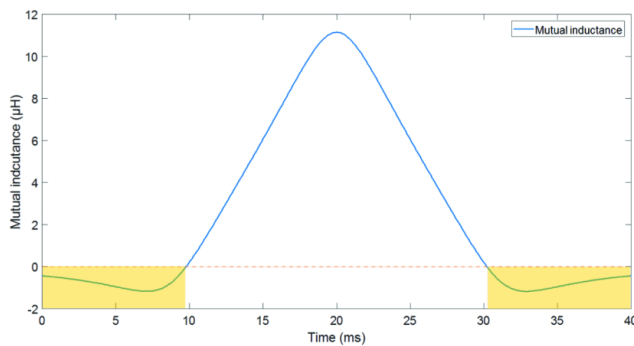


Fig. 11. Variation of the mutual inductance over time. [31]

The modelling of dynamic wireless charging has been achieved, gaining the benefit of a dynamic system response

over previous static models [32,33]. The system response shows similar characteristics to test results for dynamic inductive charging [34], further supporting the accuracy of the model. To fully verify this, the model should be set up to match physical characteristics of a test rig to best show differences in response and fully compare accuracy of the simulation vs. test results. With additional transmitter coils, the output current Figure 4 would be similar along the misalignment direction, repeated every 0.4m (coil size at 0.4m in direction of travel). The fluctuation of current would repeat in a similar fashion (with some overlap between the coils power transfer), however the output current oscillation frequency would be a function of the driving speed.

#### V. CONCLUSION

Modelling of dynamic wireless (inductive) charging has been demonstrated. The implemented system replaces previously used transformer-like approximations, using researched mutual inductance models between conductive coils. The resulting model allows easy control and change in system specifications, design and control. This paper focused on changing parameters such as coil dimensions, travel speed and ride height (air gap) in order to demonstrate the flexibility of the model. The system can be extended to include multiple transmitter and receiver coils. Coils used are approximated to a rectangular shape. The use of other shapes will required appropriate calculation adjustments, however the rest of the system remains unchanged, allowing future development for example in coil structure or materials to be easily integrated in the future.

APPENDIX

A. Mutual inductance for a pair of square coils

Using the following parameters:

$$\begin{aligned} d &= a_1 - a_2 - c & g &= a_1 - c \\ m &= a_2 + c & p &= b_1 - e \\ q &= b_2 + e & t &= b_1 - b_2 - e \end{aligned}$$

$$\begin{aligned} M &= \frac{\mu_0}{4\pi} N_1 N_2 \\ &\times \left[ \left[ d \ln \left( \frac{d + \sqrt{h^2 + (-t)^2 + d^2}}{d + \sqrt{h^2 + d^2 + q^2}} \right) \right. \right. \\ &+ h \ln \left( \frac{g + \sqrt{h^2 + q^2 + g^2}}{g + \sqrt{h^2 + g^2 + (-t)^2}} \right) \\ &+ c \ln \left( \frac{(-c) + \sqrt{h^2 + q^2 + c^2}}{(-c) + \sqrt{h^2 + c^2 + (-t)^2}} \right) \\ &+ m \ln \left( \frac{(-m) + \sqrt{h^2 + (-t)^2 + m^2}}{(-m) + \sqrt{h^2 + m^2 + q^2}} \right) \\ &+ \sqrt{h^2 + q^2 + d^2} - \sqrt{h^2 + q^2 + g^2} \\ &- \sqrt{h^2 + q^2 + m^2} + \sqrt{h^2 + q^2 + c^2} \\ &+ \sqrt{h^2 + (-t)^2 + g^2} - \sqrt{h^2 + (-t)^2 + d^2} \\ &+ \sqrt{h^2 + (-t)^2 + m^2} - \sqrt{h^2 + (-t)^2 + c^2} \left. \right] \\ &- \left[ d \ln \left( \frac{d + \sqrt{h^2 + (-p)^2 + d^2}}{d + \sqrt{h^2 + d^2 + e^2}} \right) \right. \\ &+ g \ln \left( \frac{h + \sqrt{h^2 + e^2 + g^2}}{g + \sqrt{h^2 + h^2 + (-p)^2}} \right) \\ &+ c \ln \left( \frac{(-c) + \sqrt{h^2 + e^2 + c^2}}{(-c) + \sqrt{h^2 + c^2 + (-p)^2}} \right) \\ &+ m \ln \left( \frac{(-m) + \sqrt{h^2 + (-p)^2 + m^2}}{(-m) + \sqrt{h^2 + m^2 + e^2}} \right) \\ &+ \sqrt{h^2 + e^2 + d^2} - \sqrt{h^2 + e^2 + g^2} \\ &- \sqrt{h^2 + e^2 + m^2} + \sqrt{h^2 + e^2 + c^2} \\ &+ \sqrt{h^2 + (-p)^2 + g^2} - \sqrt{h^2 + (-p)^2 + d^2} \\ &+ \sqrt{h^2 + (-p)^2 + m^2} - \sqrt{h^2 + (-p)^2 + c^2} \left. \right] \end{aligned}$$

$$\begin{aligned} &+ \left[ t \ln \left( \frac{t + \sqrt{h^2 + (-g)^2 + t^2}}{t + \sqrt{h^2 + t^2 + c^2}} \right) \right. \\ &+ p \ln \left( \frac{p + \sqrt{h^2 + p^2 + c^2}}{p + \sqrt{h^2 + (-g)^2 + p^2}} \right) \\ &+ e \ln \left( \frac{(-e) + \sqrt{h^2 + e^2 + c^2}}{(-e) + \sqrt{h^2 + e^2 + (-g)^2}} \right) \\ &+ q \ln \left( \frac{(-q) + \sqrt{h^2 + (-q)^2 + q^2}}{(-q) + \sqrt{h^2 + c^2 + q^2}} \right) \\ &+ \sqrt{h^2 + c^2 + t^2} - \sqrt{h^2 + c^2 + p^2} \\ &- \sqrt{h^2 + c^2 + q^2} + \sqrt{h^2 + e^2 + c^2} \\ &+ \sqrt{h^2 + (-g)^2 + p^2} - \sqrt{h^2 + (-g)^2 + t^2} \\ &+ \sqrt{h^2 + (-g)^2 + q^2} - \sqrt{h^2 + (-g)^2 + e^2} \left. \right] \\ &- \left[ t \ln \left( \frac{t + \sqrt{h^2 + (-d)^2 + t^2}}{t + \sqrt{h^2 + t^2 + m^2}} \right) \right. \\ &+ p \ln \left( \frac{p + \sqrt{h^2 + m^2 + p^2}}{p + \sqrt{h^2 + (-d)^2 + p^2}} \right) \\ &+ e \ln \left( \frac{(-e) + \sqrt{h^2 + e^2 + m^2}}{(-e) + \sqrt{h^2 + e^2 + (-d)^2}} \right) \\ &+ q \ln \left( \frac{(-q) + \sqrt{h^2 + (-d)^2 + q^2}}{(-q) + \sqrt{h^2 + m^2 + q^2}} \right) \\ &+ \sqrt{h^2 + m^2 + t^2} - \sqrt{h^2 + m^2 + p^2} \\ &- \sqrt{h^2 + m^2 + q^2} + \sqrt{h^2 + e^2 + m^2} \\ &+ \sqrt{h^2 + (-d)^2 + p^2} - \sqrt{h^2 + (-d)^2 + t^2} \\ &+ \sqrt{h^2 + (-d)^2 + q^2} - \sqrt{h^2 + (-d)^2 + e^2} \left. \right] \end{aligned} \tag{A1}$$

REFERENCES

- [1] U. Government, "Cop26: The negotiations explained," <https://ukcop26.org/wp-content/uploads/2021/11/COP26-Negotiations-Explained.pdf>, Nov 2021.
- [2] V. Masson-Delmotte, P. Zhai, H.-O. Pörtner, D. Roberts, J. Skea, P. R. Shukla, W. Moufouma-Okia, A. Pirani, C. Péan, R. Pidcock, S. Connors, J. B. R. Matthews, Y. Chen, X. Zhou, M. I. Gomis, E. Lonnoy, T. Maycock, M. Tignor, and T. Waterfield, "Global warming of 1.5 °c." [Online]. Available: [https://www.ipcc.ch/site/assets/uploads/sites/2/2019/06/SR15\\_Full\\_Report\\_High\\_Res.pdf](https://www.ipcc.ch/site/assets/uploads/sites/2/2019/06/SR15_Full_Report_High_Res.pdf)
- [3] C. on Climate Change, "2019 progress report to parliament," <https://www.theccc.org.uk/publication/reducing-uk-emissions-2019-progress-report-to-parliament/>, Jul 2019.
- [4] D. for Business, E. . I. Strategy, P. M. Office, . D. Street, T. R. H. K. K. MP, T. R. H. A. S. MP, and T. R. H. B. J. MP, "Uk enshrines new target in law to slash emissions by 78
- [5] D. for Business, E. . I. Strategy, and T. R. H. C. S. MP, "Uk becomes first major economy to pass net zero emissions law."
- [6] "Outcome and response to ending the sale of new petrol, diesel and hybrid cars and vans."
- [7] "Appendix g: Plug-in electric vehicle in-use and charging data analysis."
- [8] T. Chen, X.-P. Zhang, J. Wang, J. Li, C. Wu, M. Hu, and H. Bian, "A review on electric vehicle charging infrastructure development in the uk," *Journal of Modern Power Systems and Clean Energy*, vol. 8, no. 2, pp. 193–205, 2020.

- [9] H. Feng, R. Tavakoli, O. C. Onar, and Z. Pantic, "Advances in high-power wireless charging systems: Overview and design considerations," *IEEE Transactions on Transportation Electrification*, vol. 6, no. 3, pp. 886–919, 2020.
- [10] M. H. Mahtab Moon, D. Mahnaaz Mahmud, I. Ahamed, S. B. Kabir, and M. Abdul Mannan, "Static and dynamic charging system for a four-wheeler electric vehicle by inductive coupling wireless power transmission system," in *2021 International Conference on Green Energy, Computing and Sustainable Technology (GECOST)*, 2021, pp. 1–6.
- [11] Y. Liu, R. Mai, P. Yue, Y. Li, and Z. He, "Efficiency optimization for wireless dynamic charging system with overlapped dd coil arrays," in *2017 IEEE Applied Power Electronics Conference and Exposition (APEC)*, 2017, pp. 1439–1442.
- [12] M. Maemura and A. Wendt, "Dynamic power transfer as a feature - employing stationary wpt devices for dynamic operation," in *2020 IEEE PELS Workshop on Emerging Technologies: Wireless Power Transfer (WoW)*, 2020, pp. 50–55.
- [13] A. Rakhymbay, A. Khamitov, M. Bagheri, B. Alimkhanuly, M. Lu, and T. Phung, "Precise analysis on mutual inductance variation in dynamic wireless charging of electric vehicle," *Energies*, vol. 11, no. 3, 2018. [Online]. Available: <https://www.mdpi.com/1996-1073/11/3/624>
- [14] B. Song, S. Cui, Y. Li, and C. Zhu, "A fast and general method to calculate mutual inductance for ev dynamic wireless charging system," *IEEE Transactions on Power Electronics*, vol. 36, no. 3, pp. 2696–2709, 2021.
- [15] K. Hata, T. Imura, and Y. Hori, "Dynamic wireless power transfer system for electric vehicles to simplify ground facilities - power control and efficiency maximization on the secondary side," in *2016 IEEE Applied Power Electronics Conference and Exposition (APEC)*, 2016, pp. 1731–1736.
- [16] J. Sallan, J. L. Villa, A. Llombart, and J. F. Sanz, "Optimal design of icpt systems applied to electric vehicle battery charge," *IEEE Transactions on Industrial Electronics*, vol. 56, no. 6, pp. 2140–2149, 2009.
- [17] S. Y. Choi, S. Y. Jeong, E. S. Lee, B. W. Gu, S. W. Lee, and C. T. Rim, "Generalized models on self-decoupled dual pick-up coils for large lateral tolerance," *IEEE Transactions on Power Electronics*, vol. 30, no. 11, pp. 6434–6445, 2015.
- [18] M. J. Brand, M. H. Hofmann, S. S. Schuster, P. Keil, and A. Jossen, "The influence of current ripples on the lifetime of lithium-ion batteries," *IEEE Transactions on Vehicular Technology*, vol. 67, no. 11, pp. 10438–10445, 2018.
- [19] I. Puranik, L. Zhang, and J. Qin, "Impact of low-frequency ripple on lifetime of battery in mmc-based battery storage systems," in *2018 IEEE Energy Conversion Congress and Exposition (ECCE)*, 2018, pp. 2748–2752.
- [20] K. N. Mude and K. Aditya, "Comprehensive review and analysis of two-element resonant compensation topologies for wireless inductive power transfer systems," *Chinese Journal of Electrical Engineering*, vol. 5, no. 2, pp. 14–31, 2019.
- [21] K. Song, Z. Li, J. Jiang, and C. Zhu, "Constant current/voltage charging operation for series-series and series-parallel compensated wireless power transfer systems employing primary-side controller," *IEEE Transactions on Power Electronics*, vol. 33, no. 9, pp. 8065–8080, 2018.
- [22] W. Shi, F. Grazian, S. Bandyopadhyay, J. Dong, T. B. Soeiro, and P. Bauer, "Analysis of dynamic charging performances of optimized inductive power transfer couplers," in *2021 IEEE 19th International Power Electronics and Motion Control Conference (PEMC)*, 2021, pp. 751–756.
- [23] A. Caillierez, D. Sadarnac, A. Jaafari, and S. Loudot, "Dynamic inductive charging for electric vehicle: Modelling and experimental results," in *7th IET International Conference on Power Electronics, Machines and Drives (PEMD 2014)*, 2014, pp. 1–7.
- [24] Q. Zhang, S. Song, S. Dong, and C. Zhu, "Receiver-side-oriented simulator for dynamic wireless charging system with i-type transmitter and multiphase receiver," *IEEE Transactions on Industrial Electronics*, vol. 68, no. 5, pp. 3906–3916, 2021.
- [25] A. Babaki, S. Vaez-Zadeh, A. Zakerian, and G. A. Covic, "Variable-frequency retuned wpt system for power transfer and efficiency improvement in dynamic ev charging with fixed voltage characteristic," *IEEE Transactions on Energy Conversion*, vol. 36, no. 3, pp. 2141–2151, 2021.
- [26] A. Khaligh and S. Dusmez, "Comprehensive topological analysis of conductive and inductive charging solutions for plug-in electric vehicles," *IEEE Transactions on Vehicular Technology*, vol. 61, no. 8, pp. 3475–3489, 2012.
- [27] F.-S. Tsai and F. Lee, "High-frequency ac power distribution in space station," *IEEE Transactions on Aerospace and Electronic Systems*, vol. 26, no. 2, pp. 239–253, 1990.
- [28] Y. Hu, B. Ji, S. Finney, W. Xiao, and W. Cao, "High frequency inverter topologies integrated with the coupled inductor bridge arm," *IET Power Electronics*, vol. 9, no. 6, pp. 1144–1152, 2016. [Online]. Available: <https://ietresearch.onlinelibrary.wiley.com/doi/abs/10.1049/iet-pel.2014.0823>
- [29] A. Blinov, V. Ivakhno, V. Zamaruev, D. Vinnikov, and O. Husev, "Experimental verification of dc/dc converter with full-bridge active rectifier," in *IECON 2012 - 38th Annual Conference on IEEE Industrial Electronics Society*, 2012, pp. 5179–5184.
- [30] P. Davari, F. Zare, and A. Abdelhakim, "Chapter 13 - active rectifiers and their control," in *Control of Power Electronic Converters and Systems*, F. Blaabjerg, Ed. Academic Press, 2018, pp. 3–52. [Online]. Available: <https://www.sciencedirect.com/science/article/pii/B9780128161364000130>
- [31] S. Guerroudj, H. Boulzazen, and Z. Riah, "New approach for the evaluation of magnetic fields in dynamic wireless charging for electric vehicles," in *2018 IEEE International Conference on Electrical Systems for Aircraft, Railway, Ship Propulsion and Road Vehicles I& International Transportation Electrification Conference (ESARS-ITEC)*, 2018, pp. 1–5.
- [32] S. S. Biswal, D. P. Kar, and S. Bhuyan, "Consideration of series-series and series-parallel topology in perspective of dynamic resonant inductive coupling based wireless charging," in *2021 1st Odisha International Conference on Electrical Power Engineering, Communication and Computing Technology (ODICON)*, 2021, pp. 1–4.
- [33] L. Yang, B. Zhang, and M. Ju, "A fast dynamic response regulation method for undersea wireless power transfer system," in *2019 14th IEEE Conference on Industrial Electronics and Applications (ICIEA)*, 2019, pp. 1162–1166.
- [34] D. D. Snell, A. Parkes, T. Edwards, and L. Cipcigan, "Small scale multivariate testing of dynamic wireless charging," in *2020 55th International Universities Power Engineering Conference (UPEC)*, 2020, pp. 1–6.